



The effect of optimum, indication-specific imaging fields on the radiation exposure from CBCT examinations of impacted maxillary canines and mandibular third molars

Anne-Mari Ilo, Janna Waltimo-Sirén, Elmira Pakbaznejad Esmaeili, Marja Ekholm & Mika Kortesiemi

To cite this article: Anne-Mari Ilo, Janna Waltimo-Sirén, Elmira Pakbaznejad Esmaeili, Marja Ekholm & Mika Kortesiemi (2024) The effect of optimum, indication-specific imaging fields on the radiation exposure from CBCT examinations of impacted maxillary canines and mandibular third molars, *Acta Odontologica Scandinavica*, 82:1, 66-73, DOI: [10.1080/00016357.2023.2258981](https://doi.org/10.1080/00016357.2023.2258981)

To link to this article: <https://doi.org/10.1080/00016357.2023.2258981>



© 2023 The Author(s). Published by Informa UK Limited, trading as Taylor & Francis Group on behalf of Acta Odontologica Scandinavica Society.



Published online: 07 Dec 2023.



Submit your article to this journal [↗](#)



Article views: 749



View related articles [↗](#)



View Crossmark data [↗](#)

RESEARCH ARTICLE



The effect of optimum, indication-specific imaging fields on the radiation exposure from CBCT examinations of impacted maxillary canines and mandibular third molars

Anne-Mari Ilo^a, Janna Waltimo-Sirén^{b,c}, Elmira Pakbaznejad Esmaeili^d, Marja Ekholm^{a,c,d} and Mika Kortensniemi^e

^aDepartment of Oral Pathology and Oral Radiology, Institute of Dentistry, University of Turku, Turku, Finland; ^bDepartment of Pediatric Dentistry and Orthodontics, Institute of Dentistry, University of Turku, Turku, Finland; ^cWellbeing Services County of South-West Finland, Finland; ^dDepartment of Oral and Maxillofacial Diseases, University of Helsinki, Helsinki, Finland; ^eHUS Diagnostic Center, University of Helsinki and Helsinki University Hospital, Helsinki, Finland

ABSTRACT

Objective Indication-specific optimum field-of-views (FOVs) have been assessed for CBCT scans of impacted maxillary canines and mandibular third molars, as 40° × 35 mm and 35° × 35 mm, respectively. The objective was to investigate possible changes in absorbed organs and effective doses, for these two imaging indications, performing CBCT examinations with optimum FOV sizes instead of commonly used FOVs. Additionally, radiation exposure-induced cancer risk was calculated for both imaging indications with optimum FOVs.

Methods An adult female head phantom (ATOM 702-D, CIRS, Norfolk, VA, USA) was scanned using Planmeca Viso G7 CBCT-device (Planmeca, Helsinki, Finland). Scanning factors, different FOV sizes, dose-area product (DAP) values and anatomical FOV locations were used for Monte Carlo PCXMC-simulation and ImpactMC software. In the PCXMC-simulation, 10-year-old child and 30-year-old adult phantoms were used to estimating effective and absorbed organ doses.

Results The effective dose varied from 58 µSv to 284 µSv for impacted maxillary canines, and from 38 µSv to 122 µSv for mandibular third molars, the lowest dose value for each corresponding to optimum FOV. Effective dose reduction between the optimum FOV and the smallest common FOV of 50° × 50 mm, maintaining other scanning factors constant, was 33% for impacted maxillary canines, and 45% for mandibular third molars. At all examinations, the highest absorbed organ doses were in salivary glands or in oral mucosa.

Conclusions Optimum FOVs, 40° × 35 mm for impacted maxillary canine and 35° × 35 mm for mandibular third molar, could decrease effective doses received by young patients, and improve radiation safety in these common CBCT imaging procedures.

ARTICLE HISTORY

Received 4 May 2023

Revised 1 September 2023

Accepted 11 September 2023

KEYWORDS

Cone-beam computed tomography; radiation exposure; impacted; cuspid; molar; third

Introduction

Cone-beam computed tomography (CBCT) imaging modality enables three-dimensional (3D) image data with high spatial resolution from the teeth, jaw and mid-facial bony structures [1]. Localization of unerupted and impacted teeth, permanent maxillary canines and mandibular third molars in particular, is the most common imaging indication for CBCT examinations among paediatric and young adult patients [1,2]. CBCT should not, however, be a routine procedure. CBCT imaging is indicated if the clinician has a very specific clinical question that cannot be answered by conventional imaging - intraoral radiographs and panoramic tomography. Such questions include assessment of the accurate localization of an impacted maxillary canine as well as possible root resorption in adjacent teeth, and the relationship between an

unerupted mandibular third molar and the mandibular canal [3–5].

During the last decade, the popularity of CBCT imaging has increased rapidly in the dental field [6]. There has been concern about radiation exposure and patient safety because the radiation doses are generally higher in CBCT than in conventional imaging [1,7]. Moreover, the increasing number of examinations has raised the cumulative dose for patients subjected to these procedures [8]. Paediatric patients are especially vulnerable to the detrimental effects of ionizing radiation and would receive a higher effective dose than adults due to the larger anatomy covered in the CBCT scan as a result of their small size [1,9,10]. When imaging adolescents with impacted mandibular third molars, it should be taken into account that the

CONTACT Anne-Mari Ilo  anne-mari.ilo@utu.fi  Department of Oral Pathology and Oral Radiology, Institute of Dentistry, University of Turku, Lemminkäisenkatu 2, Turku, FI-20014, Finland

© 2023 The Author(s). Published by Informa UK Limited, trading as Taylor & Francis Group on behalf of Acta Odontologica Scandinavica Society.

This is an Open Access article distributed under the terms of the Creative Commons Attribution License (<http://creativecommons.org/licenses/by/4.0/>), which permits unrestricted use, distribution, and reproduction in any medium, provided the original work is properly cited. The terms on which this article has been published allow the posting of the Accepted Manuscript in a repository by the author(s) or with their consent.

effective doses are generally higher in the mandibular than in the maxillary region due to the vicinity of the thyroid gland [7, 11,12]. In addition, among children and young adults, longer life expectancy and, therefore, a higher risk for stochastic effects of radiation exposure than among older ones emphasizes the importance of radiological optimization [1,13].

Radiation dose levels in CBCT examinations vary widely mainly due to the large variability of exposure parameters, imaging field-of-view (FOV) size and geometric settings between different CBCT devices [7,9,14–16]. FOV is a cylindrical volume that determines the coverage of the patient's maxillofacial tissues exposed to the primary X-ray beam [17]. FOV size is selected according to the imaging indication and positioned with the help of anatomical landmarks before the X-ray exposure. Therefore, both the size and positioning of the FOV have a significant impact on the effective dose received by the patient [7,9,15,18]. Previous studies have highlighted that FOV selection is an important means of dose reduction, FOV should be selected according to the clinical task, and optimum indication-specific imaging protocols are needed [10, 15,16, 19]. In the literature, indication-specific optimum FOV sizes with adequate positioning have been earlier assessed for impacted maxillary canines, and mandibular third molars, as $40\varnothing \times 35$ mm and $35\varnothing \times 35$ mm, respectively [20,21]. However, the estimated absorbed organ and effective doses for performing CBCT scans with these two indication-specific FOVs have not been calculated.

SEDENTEXT guidelines recommend the calculation of absorbed organ doses and effective doses of CBCT scans by using Monte Carlo (MC) simulations [1]. MC simulation could offer a primary and accurate method for comprehensive radiation dose estimation covering organ doses compared to dosimetry measurement methods [1,22–25]. PCXMC 2.0 (Radiation and Nuclear Safety Authority, Helsinki, Finland) is an MC-based software that allows the calculation of organ doses based on an anatomic phantom model and exposure parameters including X-ray spectrum and dose-area product (DAP) or incident air-kerma applied to rotational CBCT exposure [23]. Based on the simulated organ doses, the program enables the calculation of the effective doses by using tissue weighting factors based on International Commission on Radiological Protection (ICRP) publication 103 [26] or 60 [27]. Furthermore, radiation risk estimation can be calculated according to the sex- and age-dependent cancer risk model of the BEIR VII (Biologic Effects of Ionizing Radiation VII) committee [28].

In this study, MC simulations were performed regarding CBCT imaging of impacted maxillary canines and mandibular third molars. The objective was to investigate how and to what extent CBCT examinations performed using earlier-defined indication-specific optimum FOV sizes, of $40\varnothing \times 35$ mm and $35\varnothing \times 35$ mm, instead of commonly used larger FOV sizes, differ in terms of absorbed organ and effective doses. Additionally, radiation exposure-induced cancer risk was calculated for both the above-mentioned imaging indications with optimum FOV sizes.

Materials and methods

CBCT unit, phantom and scanning parameters

CBCT examinations were performed using the Planmeca Viso G7 CBCT-scanner (Planmeca, Helsinki, Finland) at HUS Surgical Hospital of Helsinki University Hospital, Helsinki, Finland. The device has capable FOV sizes ranging from $30\varnothing \times 30$ mm to $260\varnothing \times 300$ mm. In this study, in terms of impacted maxillary canines and mandibular third molars, the most clinically used different FOV sizes were manually selected to include $35\varnothing \times 35$ mm, $40\varnothing \times 35$ mm, $50\varnothing \times 50$ mm, $70\varnothing \times 80$ mm, $80\varnothing \times 50$ mm, and $100\varnothing \times 100$ mm. The larger FOV sizes, $140\varnothing \times 100$ mm and $260\varnothing \times 300$ mm, were included as reference imaging fields.

X-ray tube voltage, tube current and exposure time values were in automatic settings. At all exposures, the standard patient size, M, was chosen from a scale of XS to XL in the device. Voxel sizes were in automatic settings, $150\mu\text{m}$ or $450\mu\text{m}$, with one exception: when scanning impacted maxillary canine with $40\varnothing \times 35$ mm FOV, the voxel sizes were the automatic $150\mu\text{m}$ and a manually selected $75\mu\text{m}$. The largest FOVs ($140\varnothing \times 100$ mm and $260\varnothing \times 300$ mm) had a larger voxel size of $450\mu\text{m}$. The used degree of rotation of the scanner was 210° . Anode angle of the X-ray tube was 10° , and total filtration $2.5\text{ mm Al} + 0.5\text{ mm Cu}$.

CBCT examinations were performed by orientating a head and neck part of an adult female anthropomorphic phantom (ATOM 702-D, CIRS, Norfolk, VA, USA) in the stand-up position, as used in the patient examination. The head and neck part of the phantom is 22.5 cm long in z-direction (including nine 2.5 cm physical sections) and composed of tissue equivalent materials, epoxy resins and polymers, to mimic any tissues in the human body. Bone tissue of the phantoms is formulated with age-related density [29,30].

The tooth-specific FOV placement was made by using Romexis software (Planmeca, Helsinki, Finland). A center of the FOV was positioned according to indication and adjusted, if necessary, based on a scout view. DAP value, expressed in mGy cm^2 , was reported after each radiation exposure on the device panel.

Radiation output of the CBCT-device was ensured by measuring air-kerma value with calibrated Raysafe X2 R/F dosimeter (Unfors RaySafe AB, Billdal, Sweden). The dosimeter was set on the surface of a device detector and the measurement was performed with $100\varnothing \times 100$ mm FOV scanning protocol using 100 kV , 12.5 mA tube current and 5 s exposure time (63 mAs), as applied in clinical scans. The measured air-kerma value was converted to DAP by applying distance correction to isocenter and multiplying by beam area at isocenter.

Simulation programs

The DAP values and anatomical FOV-position data were entered into PCXMC 2.0 rotation version simulation program to estimate absorbed organ and effective doses of the CBCT-scans. In simulation software, a 10-year-old virtual phantom was used to estimate dose values for impacted maxillary

Table 1. Reference location center points of the PCXMC simulations for different sizes of field-of-view (FOV) on maxillary canines and mandibular third molars.

Target	FOV (mm) (diameter x height)	Xref (cm)	Yref (cm)	Zref (cm)
Canine (left)	Ø 40 × 35	3	-6.5	60.0
	Ø 50 × 50	3	-6.5	60.0
	Ø 70 × 80	1	-6.0	58.5
Canines (both)	Ø 80 × 50	0	-6.0	58.5
	Ø 100 × 100	0	-6.0	58.5
Third molar (left)	Ø 35 × 35	5	-3.0	82.0
	Ø 50 × 50	4	-3.0	82.0
	Ø 70 × 80	4	-3.0	82.0
Third molars (both)	Ø 80 × 50	0	-3.0	83.0
	Ø 140 × 100	0	-3.0	82.0
Whole skull	Ø 260 × 300	0	-1.0	87.0

canines, and an adult phantom for impacted mandibular third molars. The coordinate system of the program is based on the central axis of the X-ray beam: the positive z-axis points upwards, the x-axis to the left-hand side and the positive y-axis to the back of the phantom. Zero points of the x- and y-axes is in the centerline of the skull in the modified Cristy and Eckerman phantom model of the program. Reference points of the different FOV sizes are shown in Table 1. Focus to isocenter distance was 41 cm. X-ray beam width and height varied according to the applied FOV size.

Moreover, two comparative exposure scenarios and corresponding effective doses for the optimum imaging field (40Ø × 35 mm) of left maxillary canine were calculated by varying the reference 100 kV tube voltage by applying 90 kV (lower voltage) and 110 kV (higher voltage). Standardized DAP value (151 mGy cm²) was maintained in these comparative simulations. The 90 kV simulation also was used to calculate doses from ultra-low-dose (ULD) scan where half of the regular mAs is applied. A voltage value 90 kV corresponded to a standard scan for a child (XS) and small (S) adult, and 110 kV to large (L) adult scan.

In PCXMC 2.0 program, the estimated organ and effective doses were based on tissue weighting factors reported by ICRP publication 103 [26]. Sensitivity analyses were performed for the effective doses of optimum imaging fields, 40Ø × 35 mm FOV size for impacted maxillary canines and 35Ø × 35 mm for mandibular third molars, with variable FOV positions. The FOV position translated ± 1 cm along x-, y- and z-axes from the reference location. Thus, six dose simulations were performed and compared to corresponding (canine and third molar) reference simulations in sensitivity analyses.

In addition to the PCXMC simulations, ImpactMC software (ImpactMC, Vamp GmbH, Germany) was used to visualize 3D radiation dose distribution of optimum FOV separately for impacted maxillary canine and mandibular third molar. The CT scan data of the ATOM anthropomorphic phantom was used as the patient model input data and the applied CBCT scan parameters were used to configure the X-ray source parameters in the simulation. X-ray source spectrum was separately calculated with Spekcalc 2.0 program for the 3D dose simulation [31].

Demonstrative cancer risk estimation for impacted maxillary canines and mandibular third molars were calculated from the optimum FOV scans (40Ø × 35 mm and 35Ø × 35 mm), by

using BEIR VII committee risk model [28]. The risk calculations were performed for 10-year-old Euro-American girl and boy with impacted maxillary canine, and for 30-year-old Euro-American female and male with impacted mandibular third molar, taking into account the simulated organ doses.

Results

Impacted maxillary canines

Simulated effective doses (E), absorbed organ doses, E/DAP ratios and entrance surface air-kerma (ESAK) values at scan isocenter for different FOV sizes, at 100 kV and 150 µm voxel size, are shown in Table 2. The effective doses varied from 58 µSv to 284 µSv for impacted maxillary canines, and the lowest dose value was achieved with optimum, 40Ø × 35 mm, FOV size. Effective dose reduction between the optimum FOV and the smallest common FOV of 50Ø × 50 mm was 33%.

Regarding the effect of other parameters, comparative effective doses from the optimum 40Ø × 35 mm FOV size for left impacted maxillary canine were simulated by using different voltage values corresponding with standard patient size models. Selected voltage values were 90 kV (child, XS, and small adult, S), 90 kV and halved mAs (ULD scan), 100 kV (medium adult, M) and 110 kV (large adult, L), and respective estimated effective dose were 56 µSv, 28 µSv, 58 µSv, and 59 µSv.

When retaining the optimum FOV size 40Ø × 35 mm and voltage of 100 kV constant but using voxel size 75 µm instead of 150 µm, the effective dose increased from 58 µSv to 91 µSv. If FOV 80Ø × 50 mm were selected to include both right- and left-side maxillary canines, the estimated effective dose was 147 µSv, which is higher than the total dose from two separate CBCT scans of 40Ø × 35 mm. However, bilaterally impacted maxillary canines would, occasionally, be covered by FOV of 50Ø × 50 mm, resulting in an estimated effective dose of 87 µSv.

In terms of the left maxillary canine, the highest absorbed organ doses were measured in salivary glands and oral mucosa, followed by thyroid, brain, and esophagus, with all FOV-size variations. When regarding absorbed doses specifically in the thyroid, the lowest value, 110 µGy, was achieved with 40Ø × 35 mm FOV size, and the highest value, 1671 µGy, with the largest, 100Ø × 100 mm FOV (Table 2). Radiation distribution for left maxillary canine with 40Ø × 35 mm FOV is illustrated in Figures 1(a–c).

As a demonstrative radiation risk calculation, the risk of exposure-induced cancer death with optimum FOV size, 40Ø × 35 mm, (DAP = 151 mGy cm², E = 58 µSv) was 0.00015% and loss of life expectancy 0.5 h taking into account organ doses and assuming patient model of a 10-year-old Euro-American girl. For a boy of the same age, the risk values were 0.00013% and 0.4 h, respectively.

Impacted mandibular third molars

In the simulated imaging of mandibular third molars, estimated effective dose values varied between 38 µSv and 122

Table 2. Simulated effective and absorbed organ doses from CBCT examinations of impacted maxillary canines and mandibular third molars.

Target	FOV (mm) (diameter x height)	Voxel size(µm)	Scanning parameters				Radiation doses				Organ doses (µGy)			
			Voltage(kV)	Current(mA)	Exposure time(s)	DAP(mGy cm ²)	ESAK* (mGy)	Effective dose** E(µSv)	Ratio E/ DAP(µSv/ mGy cm ²)	Thyroid	Brain	Salivary glands	Esophagus	Oral mucosa
Canine (left)	Ø 40×35	150	100	12.5	5.04	151	10.8	58	0.384	110	104	1043	7	1709
	Ø 40×35	75	100	12.5	8.00	237	16.9	91	0.384	172	163	1637	11	2683
	Ø 50×50	150	100	12.5	5.04	245	9.8	87	0.355	181	180	1605	12	2458
Canines (both)	Ø 70×80	150	100	12.5	5.04	506	9.0	183	0.362	718	284	3816	41	3928
	Ø 80×50	150	100	12.5	5.04	371	9.3	147	0.396	463	180	3399	30	3933
	Ø 100×100	150	100	12.5	5.04	847	8.5	284	0.335	1671	566	5326	65	4902
Third molar (left)	Ø 35×35	150	100	12.5	5.04	135	11.0	38	0.281	48	48	1441	3	1110
	Ø 50×50	150	100	12.5	5.04	245	9.8	69	0.282	103	98	2461	5	1900
	Ø 70×80	150	100	12.5	5.04	506	9.0	122	0.241	224	225	4150	10	2819
Third molars (both)	Ø 80×50	150	100	12.5	5.04	371	9.3	96	0.259	116	218	2741	6	2917
	Ø 140×100	450	100	12.5	2.56	398	2.8	75	0.188	164	209	2175	8	1585
Whole skull	Ø 260×300	450	100	10.0	3.20	1370	1.7	115	0.084	703	1486	1628	19	1147

FOV: Field-of-view, DAP: Dose-area product; ESAK: Entrance surface air-kerma at scan isocenter (without scatter).

*ESAK is calculated according to displayed DAP and FOV area (in cm²) at isocenter.

**Effective dose is simulated.

µSv (Table 2). The lowest dose value was achieved with the optimum FOV size, 35Ø × 35mm. Effective dose reduction between the optimum and 50Ø × 50mm FOV sizes was 45%. FOV size of 80Ø × 50mm, or a larger FOV, depending on the size of the mandible, could be selected to include the mandibular third molars bilaterally. An alternative option is to choose two small FOV sizes separately for the right and left sides. Selection of FOV size 80Ø × 50mm yielded an effective dose of 96 µSv, whereas the simulated usage of optimum 35Ø × 35mm FOV separately for right and left sides gave a lower total dose of 76 µSv, favouring the common clinical practice of two separate exposures.

Salivary glands achieved the highest absorbed organ doses with every FOV size, except one, 80Ø × 50mm, which targets the highest organ dose in the oral mucosa. In terms of the thyroid gland, the lowest absorbed dose, 48 µGy, was achieved with optimum FOV size and the highest, 224 µGy, with 70Ø × 80mm FOV. Absorbed organ doses are also shown in Table 2. Radiation distribution for the left mandibular third molar with 35Ø × 35mm FOV is illustrated in Figures 1(d-f).

As a demonstrative radiation risk calculation, the risk of exposure-induced cancer death with optimum FOV size, 35Ø × 35mm, (DAP = 135 mGy cm², E=38 µSv) was 0.000041% and loss of life expectancy 0.1h taking into account organ doses and assuming patient model of a 30-year-old Euro-American female. For a 30-year-old male, the value of radiation-induced cancer death was 0.000039%, and loss of life expectancy, rounded to one significant figure, was the same as for a female.

Sensitivity analysis of optimum FOV position

In the maxilla, when using the optimum FOV size for impacted maxillary canine, the effective dose values ranged between 51 µSv and 60 µSv by relocating FOV position 1 cm from the center point in turn into six different directions in xyz-coordinate (Table 3a). The greatest change, 7 µSv reduction, resulted from repositioning FOV 1 cm up (more cranially) along z-axis (Zref + 1 cm). In the mandibular third molar area, the range of effective dose was 35 – 41 µSv with repositioning of the 35Ø × 35mm FOV size (Table 3b). On x-axis, 1 cm position translation to the right or left had no effect on the effective dose. On y- and z-axes, effective doses varied slightly, 1-3 µSv.

Discussion

The purpose of this study was to define the effect of different FOV sizes on the estimated effective and absorbed organ doses attained from dental CBCT examinations of impacted maxillary canines and mandibular third molars. Indication-specific optimum FOV sizes, which have been assessed for these two CBCT imaging indications [20,21], were a special focus. Monte Carlo simulations were applied to calculate radiation dose distributions, mean organ and effective doses, and radiation-related cancer risks.

All dose estimation methods have certain limitations inherent to methodology and systematic assumptions such

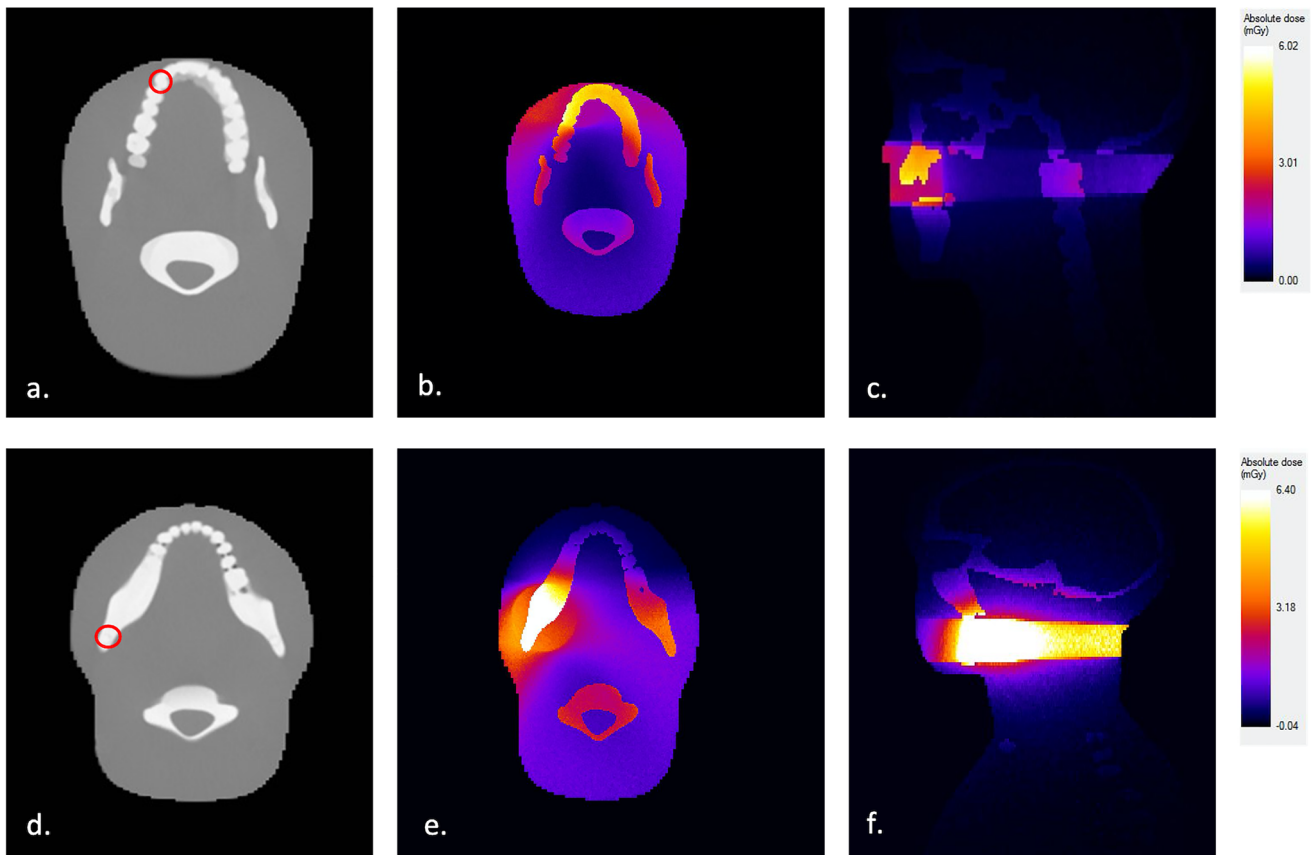


Figure 1. Monte Carlo (ImpactMC) simulation of the 3D radiation dose distribution for CBCT scans of impacted maxillary canines and mandibular third molars with $40\text{Ø} \times 35\text{ mm}$ FOV as applied to ATOM anthropomorphic female adult head and neck phantom model. **(a)** Imaging field positioning according to the location of a left maxillary canine tooth. **(b)** Simulated radiation dose distribution in axial view and **(c)** sagittal view for impacted maxillary canine, presented as a relative color heatmap. **(d)** Imaging field positioning according to the location of a left mandibular third molar tooth. **(e)** Simulated radiation dose distribution in axial view and **(f)** sagittal view for impacted mandibular third molar, presented as a relative color heatmap.

Table 3. Results of sensitivity analysis simulation with variable positioning of minimum FOV.

a. Position translations of $40\text{Ø} \times 35\text{ mm}$ FOV for left impacted maxillary canine (DAP 151 mGy cm^2, voxel size $150\text{ }\mu\text{m}$)			
Effective dose (E)		58 μSv	
FOV position translation on x-axis	x -1 cm (right/in)	x +1 cm (left/out)	
E	60 μSv	54 μSv	
Ratio	1.03	0.93	
FOV position translation on y-axis	y -1 cm (front/out)	y +1 cm (back/in)	
E	53 μSv	60 μSv	
Ratio	0.91	1.03	
FOV position translation on z-axis	z -1 cm (down)	z +1 cm (up)	
E	59 μSv	51 μSv	
Ratio	1.02	0.88	
b. Position translations of $35\text{Ø} \times 35\text{ mm}$ FOV for left impacted mandibular third molar (DAP 135 mGy cm^2, voxel size $150\text{ }\mu\text{m}$)			
Effective dose (E)		38 μSv	
FOV position translation on x-axis	x -1 cm (right/in)	x +1 cm (left/out)	
E	38 μSv	38 μSv	
Ratio	1.00	1.00	
FOV position translation on y-axis	y -1 cm (front/out)	y +1 cm (back/in)	
E	36 μSv	39 μSv	
Ratio	0.95	1.03	
FOV position translation on z-axis	z -1 cm (down)	z +1 cm (up)	
E	35 μSv	41 μSv	
Ratio	0.92	1.08	

as patient model and organ shapes, sizes and locations. This is where the limitations and main uncertainties of dose estimates can be anticipated in our study as well. The reported mean age of children undergoing CBCT procedures due to impacted maxillary canines is around 12 years [20], whereas

the simulation in the present study was performed on a 10-year-old phantom. Significant variations of anatomical size and morphology can, however, be anticipated for any pediatric age group. Thus, any radiation exposure simulation or measurement involving a specific patient model should be

interpreted with caution when using such results in the assessment of radiation exposure to any specific patient population. Furthermore, the effective dose is calculated for a reference human model and serves as a comparative radiation protection quantity; it is not an accurate radiation exposure estimate for any specific population or individual [32]. PCXMC-simulation software includes uncertainty estimation for calculated dose quantities. The statistical error is usually a small uncertainty factor, shown in percentages, among the total uncertainty of the results, where the differences between simulated and real patient geometry will often dominate [33].

Our study also included an assessment of risk estimates. More specifically, the risk of exposure-induced death (REID) values of 10-year-old were approximately triple compared to the values of a 30-year-old. A previous publication reports REID values of 22.6×10^{-7} and 19×10^{-7} for 10-year-old females and male, and 10.4×10^{-7} and 8.88×10^{-7} for 30-year-old females and males, respectively [34]. Although the risk values found in the present study were somewhat higher, they are all in all, extremely low when considering the overall cancer risk from other sources. Yet it is noticeable that a child with impacted maxillary canine may undergo several CBCT procedures, unlike a young adult with mandibular third molars, due to follow-up of canine eruption or root resorption of the adjacent teeth. Therefore, optimization of particularly canine imaging is important.

Reduction of canine imaging FOV from the commonly used small $50 \text{ } \varnothing \times 50 \text{ mm}$ into our suggested optimum FOV of $40 \text{ } \varnothing \times 35 \text{ mm}$ [20] lowered the effective dose by 33%. Regarding imaging of mandibular third molars, a similar replacement of the small FOV by our suggested optimum FOV of $35 \text{ } \varnothing \times 35 \text{ mm}$ [21] reduced the effective dose by 45%. It is important to recognize that dose values between these two imaging indications are not comparable with each other, but only within the same imaging indication. In the clinical aspect, the applied optimum indication-specific FOV sizes are not standard, pre-set FOV volumes in CBCT-devices, and the usage of these volumes requires more seamless and flexible adjustability of FOV than all CBCT devices could yet offer. Favourably, an improvement in FOV adjustability is one development trend introduced in new CBCT scanners. Already, some new CBCT devices utilize freely adjustable FOV systems from $20 \text{ } \varnothing \times 20 \text{ mm}$ to full craniofacial imaging, making the usage of more flexible indication-specific FOV sizes possible in practice [35].

The selection of low-dose CBCT scan protocol with half of the regular mAs and optimum FOV size for impacted maxillary canines decreased further the effective dose value from $58 \text{ } \mu\text{Sv}$ to $28 \text{ } \mu\text{Sv}$. Previous studies have reported a wide variation of effective doses in canine regions [9,15,36]. In an earlier study by Marcu et al. estimated radiation doses of CBCT scans with different FOV sizes for pediatric patients ranged between 18 to $218 \text{ } \mu\text{Sv}$ [15]. The lowest dose was achieved with an 8-year-old pediatric phantom by using a low-dose CBCT scan protocol combined with a small FOV size, $42 \text{ } \varnothing \times 55 \text{ mm}$ [15]. The dose is slightly lower than the smallest dose of $28 \text{ } \mu\text{Sv}$ observed in the present simulation with low-dose protocol, applying an even smaller FOV on a slightly older phantom model. In terms of using a normal protocol and

$50 \text{ } \varnothing \times 50 \text{ mm}$ FOV size, our result, $87 \text{ } \mu\text{Sv}$, was in very good agreement with the study by Kadesjö et al. where the estimated effective dose for impacted canine was $88 \text{ } \mu\text{Sv}$ by using a pediatric 10-year-old anthropomorphic phantom with $40 \text{ } \varnothing \times 50 \text{ mm}$ FOV size [36]. The present lowest effective dose for impacted mandibular third molars was $38 \text{ } \mu\text{Sv}$, and it was achieved with optimum FOV size. In the mandibular third molar region, and for adults, earlier reported effective doses were $75.3 \text{ } \mu\text{Sv}$ with $60 \text{ } \varnothing \times 60 \text{ mm}$ FOV [12] and $41 \text{ } \mu\text{Sv}$ with $40 \text{ } \varnothing \times 40 \text{ mm}$ [8] making our results with small FOV sizes consistent with previous studies.

When imaging impacted maxillary canines with CBCT, higher resolution facilitates a better interpretation of root resorption of adjacent teeth [15,37]. In our study, the higher resolution, voxel size $75 \text{ } \mu\text{m}$ instead of $150 \text{ } \mu\text{m}$, increased the effective dose value from $58 \text{ } \mu\text{Sv}$ to $91 \text{ } \mu\text{Sv}$ with the optimum FOV of $40 \text{ } \varnothing \times 35 \text{ mm}$. The dose value with the higher resolution was, however, lower than an earlier reported effective dose value $125 \text{ } \mu\text{Sv}$ with a normal dose protocol and high resolution for an 8-year-old with impacted canines [15]. In the literature, voxel sizes $100 \text{ } \mu\text{m} - 200 \text{ } \mu\text{m}$ are preferred when assessing root resorption from CBCT scans [37,38], and, according to SEDENTEXCT guidelines, CBCT examinations should apply the largest voxel size (lowest dose) consistent with acceptable diagnostic accuracy [1]. The clinical importance of high-resolution imaging of impacted maxillary canines remains questionable, since if canine-induced resorption of the incisor roots is not severe, the long-term prognosis of teeth is good despite some root resorption [39], and hence any root resorption of evidence-based significance for clinical decision making will not remain undetected with normal $200 \text{ } \mu\text{m}$ voxel size.

In our study, the salivary glands and oral mucosa received the highest organ doses in all studied scans. It is worth noting that absorbed organ doses are relatively similar between these two tissues despite the difference in tissue weighting factors according to ICRP publication 103 [26]. The weighting factor for salivary glands is 0.01 and for oral mucosa 0.12 (is included in the remaining organs) [26]. The reason for the high absorbed doses of salivary glands is the closer location to the primary X-ray beam. Comparing organ doses absorbed by salivary glands and the thyroid, the more caudal (*i.e.* lower) location of the thyroid resulted in relatively lower organ doses, although the tissue weighting factor is higher, 0.04 [26]. Nevertheless, in this study, CBCT scans of the canine region led to higher absorbed doses in the thyroid than scans of the third molar region due to the selected ages of the phantom models. This is consistent with earlier studies; the pediatric model exhibits smaller anatomical size with the potentially closer location of radiosensitive organs to the primary radiation beam compared to an adult one with the same applied FOV sizes [1,9]. Thus, the specific contribution of organ dose to the effective dose is dependent on scanning parameters in each indication-specific CBCT scan with significant differences between indications and available scan settings in various CBCT equipment models [9,15,24,34,40].

Diagnostic reference dose levels (DRLs) have proven to be practical basic tools for the optimization of medical exposures in radiology [41]. DRL quantities should be appropriate to the

imaging method, and in dental CBCT, DRLs are expressed in DAP values [1,41]. Hidalgo-Rivas et al. reported DAP value of 146 mGy cm² in CBCT examination of the anterior maxilla with low-dose protocol for pediatric patients, which is close to what we found (151 mGy cm²) as the lowest corresponding DAP value in our study [10]. However, equal DAP values can be achieved with different exposure parameters and FOV locations, and therefore more comprehensive dosimetric evaluation is required when a more accurate estimate of the radiation exposure of the patient is needed (involving organ doses and effective doses) [14]. Nevertheless, DRLs are valuable basic guides for self-assessment in dose optimization in the clinical environment. Further studies could include research about the most commonly used FOV sizes and general radiation doses, in practice, from CBCT imaging of impacted maxillary canines and mandibular third molars in different dental clinics. Such data would be valuable when formulating further national guidelines, preferably with DRLs for common CBCT imaging indications, and in identifying special needs of continuous education in radiation protection.

Conclusion

The present study demonstrated that the estimated effective doses attained from CBCT scans can be decreased by using indication-specific optimum FOV sizes, 40° × 35 mm for impacted maxillary canines and 35° × 35 mm for mandibular third molars, instead of commonly used small FOV size of 50° × 50 mm, by 33% and 45%, respectively. In a clinical aspect, if a CBCT scanner utilizes freely adjustable FOV systems, the use of these indication-specific FOV sizes, maintaining other scanning factors standards, could improve the radiation protection of a patient in CBCT imaging procedure.

Ethical approval

Not applicable. This article does not contain any studies with human or animal subjects performed by any of the authors.

Disclosure statement

No potential conflict of interest was reported by the author(s).

Funding

This study was funded by a personal grant from The Finnish Dental Society to Anne-Mari Ilo.

References

- [1] SEDENTEXCT Radiation protection no 172. Cone beam CT for dental and maxillofacial radiology. Evidence-based guidelines. Luxembourg: European Commission. 2012. [cited 2022 Jan 9]. Available from: http://www.sedentext.eu/files/radiation_protection_172.pdf.
- [2] İşman Ö, Yılmaz HH, Aktan AM, et al. Indication for cone beam computed tomography in children and young patients in a Turkish subpopulation. *Int J Paediatr Dent*. 2017;27(3):183–190. doi: 10.1111/ipd.12250.
- [3] Horner K, Barry S, Dave M, et al. Diagnostic efficacy of cone beam computed tomography in paediatric dentistry: a systematic review. *Eur Arch Paediatr Dent*. 2020;21(4):407–426. doi: 10.1007/s40368-019-00504-x.
- [4] Matzen L, Berkhout E. Cone beam CT imaging of the mandibular third molar: a position paper prepared by the European Academy of DentoMaxillofacial Radiology (EADMFR). *Dentomaxillofac Radiol*. 2019;48(5):20190039. doi: 10.1259/dmfr.20190039.
- [5] Kühnisch J, Anttonen V, Duggal MS, et al. Best clinical practice guidance for prescribing dental radiographs in children and adolescents: an EAPD policy document. *Eur Arch Paediatr Dent*. 2020;21(4):375–386. doi: 10.1007/s40368-019-00493-x.
- [6] Radiation and Nuclear Safety Authority in Finland. Radiologisten tutkimusten ja toimenpiteiden määrät vuonna 2018. STUK-B:242. 2019. [cited 2020 March 25]. Available from: <http://urn.fi/URN:ISBN:978-952-309-449-9>
- [7] Ludlow JB, Timothy R, Walker C, et al. Effective dose of dental CBCT – a meta-analysis of published data and additional data of nine CBCT units. *Dentomaxillofac Radiol*. 2015;44(7):20159003. doi: 10.1259/dmfr.20159003.
- [8] Mutalik S, Tadinada A, Molina MR, et al. Effective doses of dental cone beam computed tomography: effect of 360-degree versus 180-degree rotation angles. *Oral Surg Oral Med Oral Pathol Oral Radiol*. 2020;130(4):433–446. doi: 10.1016/j.oooo.2020.04.008.
- [9] Almuqrin AH, Tamam N, Abdelrazig A, et al. Organ dose and radiogenic risk in dental cone-beam computed tomography examinations. *Radiat Phys Chem*. 2020;176:108971. doi: 10.1016/j.radphyschem.2020.108971.
- [10] Hidalgo Rivas JA, Horner K, Thiruvengkatachari B, et al. Development of a low-dose protocol for cone beam CT examinations of the anterior maxilla in children. *Br J Radiol*. 2015;88(1054):20150559. doi: 10.1259/bjr.20150559.
- [11] Kralik I, Faj D, Lauc T, et al. Dose area product in estimation of effective dose of the patients undergoing dental cone beam computed tomography examinations. *J Radiol Prot*. 2018;38(4):1412–1427. doi: 10.1088/1361-6498/aae4e8.
- [12] Roberts JA, Drage NA, Davies J, et al. Effective dose from cone beam CT examinations in dentistry. *Br J Radiol*. 2009;82(973):35–40. doi: 10.1259/bjr/31419627.
- [13] Ludlow JB, Walker C. Assessment of phantom dosimetry and image quality of i-CAT FLX cone-beam computed tomography. *Am J Orthod Dentofacial Orthop*. 2013;144(6):802–817. doi: 10.1016/j.ajodo.2013.07.013.
- [14] Pauwels R, Theodorakou C, Walker A, et al. Dose distribution for dental cone beam CT and its implication for defining a dose index. *Dentomaxillofac Radiol*. 2012;41(7):583–593. doi: 10.1259/dmfr/20920453.
- [15] Marcu M, Hedesiu M, Salmon B, DIMITRA Research Group, et al. Estimation of the radiation dose for pediatric CBCT indications: a prospective study on ProMax3D. *Int J Paediatr Dent*. 2018;28(3):300–309. doi: 10.1111/ipd.12355.
- [16] Jadu FM, Alzahrani AA, Almutairi MA, et al. The effect of varying cone beam computed tomography image resolution and field-of-view centralization on effective radiation dose. *Saudi Med J*. 2018;39(5):470–475. doi: 10.15537/smj.2018.5.21658.
- [17] Lofthag-Hansen S, Thilander-Klang A, Ekstubby A, et al. Calculating effective dose on a cone beam computed tomography device: 3D accuitomo and 3D accuitomo FPD. *Dentomaxillofac Radiol*. 2008; 37(2):72–79. doi: 10.1259/dmfr/60375385.
- [18] Kim IH, Singer SR, Mupparapu M. Review of cone beam computed tomography guidelines in North America. *Quintessence Int*. 2019;50:136–145. [cited 2020 Dec 30]. Available from <https://www.quintessence-partner.com/cone-beam-computed-tomography-guidelines/>
- [19] Choi E, Ford NL. Measuring absorbed dose for i-CAT CBCT examinations in child, adolescent and adult phantoms. *Dentomaxillofac Radiol*. 2015;44(6):20150018. doi: 10.1259/dmfr.20150018.

- [20] Pakbaznejad Esmaeili E, Ilo A-M, Waltimo-Sirén J, et al. Minimum size and positioning of imaging field for CBCT scans of impacted maxillary canines. *Clin Oral Investig*. 2020;24(2):897–905. doi: [10.1007/s00784-019-02904-1b](https://doi.org/10.1007/s00784-019-02904-1b).
- [21] Ilo A-M, Ekholm M, Pakbaznejad Esmaeili E, et al. Minimum size and positioning of imaging field for CBCT-scans of impacted lower third molars: a retrospective study. *BMC Oral Health*. 2021;21(1):670. doi: [10.1186/s12903-021-02029-6](https://doi.org/10.1186/s12903-021-02029-6).
- [22] Vassileva J, Stoyanov D. Quality control and patient dosimetry in dental cone beam CT. *Radiat Prot Dosimetry*. 2010;139(1-3):310–312. doi: [10.1093/rpd/ncq011](https://doi.org/10.1093/rpd/ncq011).
- [23] International Commission on Radiation Units and Measurements (ICRU). Patient dosimetry for x-rays used in medical imaging report no. J ICRU. 2005;5(74):2.
- [24] Kim EK, Han WJ, Choi JW, et al. Estimation of the effective dose of dental cone-beam computed tomography using personal computer-based monte carlo software. *Imaging Sci Dent*. 2018;48(1):21–30. doi: [10.5624/isd.2018.48.1.21](https://doi.org/10.5624/isd.2018.48.1.21).
- [25] Lee C, Yoon J, Han S-S, et al. Dose assessment in dental cone-beam computed tomography: comparison of optically stimulated luminescence dosimetry with Monte Carlo method. *PLoS One*. 2020;15(3):e0219103. doi: [10.1371/journal.pone.0219103](https://doi.org/10.1371/journal.pone.0219103).
- [26] ICRP. The 2007 recommendations of the international commission on radiological protection. *Ann ICRP*. 2007;37:2–4. ICRP publication 103
- [27] ICRP. 1991. The 1990 recommendations of the international commission on radiological protection. ICRP publication 103. *Ann ICRP* 37 (2-4)
- [28] National Research Council. Health risks from exposure to low levels of ionizing radiation. : BEIR VII Phase 2. Washington, DC: the National Academies Press; 2006.
- [29] ICRP. 1975. Report of the Task Group on Reference Man. ICRP Publication 23. Pergamon Press, Oxford.
- [30] Woodard HQ, White DR. The composition of body tissues. *Br J Radiol*. 1986;59(708):1209–1218. doi: [10.1259/0007-1285-59-708-1209](https://doi.org/10.1259/0007-1285-59-708-1209).
- [31] Poludniowski G, Landry G, DeBlois F, et al. SpekCalc: a program to calculate photon spectra from tungsten anode x-ray tubes. *Phys Med Biol*. 2009;54(19):N433–8. doi: [10.1088/0031-9155/54/19/n01](https://doi.org/10.1088/0031-9155/54/19/n01).
- [32] Fisher DR, Fahey FH. Appropriate use of effective dose in radiation protection and risk assessment. *Health Phys*. 2017;113(2):102–109. doi: [10.1097/hp.0000000000000674](https://doi.org/10.1097/hp.0000000000000674).
- [33] Tapiovaara M, Siiskonen T. PCXMC 2.0: user's Guide. 2008. [cited 2023 March 1]. Available from: <https://www.stuk.fi/documents/12547/474783/stuk-tr7.pdf/6f42383b-be6d-468a-9a00-a49ca8c9ef31>.
- [34] Yeh JK, Chen CH. Estimated radiation risk of cancer from dental cone-beam computed tomography imaging in orthodontics patients. *BMC Oral Health*. 2018;18(1) doi: [10.1186/s12903-018-0592-5](https://doi.org/10.1186/s12903-018-0592-5).
- [35] Kaasalainen T, Ekholm M, Siiskonen T, et al. Dental cone beam CT: an updated review. *Phys Med*. 2021;88:193–217. doi: [10.1016/j.ejmp.2021.07.007](https://doi.org/10.1016/j.ejmp.2021.07.007).
- [36] Kadesjö N, Lynds R, Nilsson M, et al. Radiation dose from X-ray examinations of impacted canines: cone beam CT vs two-dimensional imaging. *Dentomaxillofac Radiol*. 2018;47(3):20170305. doi: [10.1259/dmfr.20170305](https://doi.org/10.1259/dmfr.20170305).
- [37] da Silveira PF, Fontana MP, Oliveira HW, et al. CBCT-based volume of simulated root resorption - influence of FOV and voxel size. *Int Endod J*. 2015;48(10):959–965. doi: [10.1111/iej.12390](https://doi.org/10.1111/iej.12390).
- [38] Spin-Neto R, Gotfredsen E, Wenzel A. Impact of voxel size variation on CBCT-based diagnostic outcome in dentistry: a systematic review. *J Digit Imaging*. 2013;26(4):813–820. doi: [10.1007/s10278-012-9562-7](https://doi.org/10.1007/s10278-012-9562-7).
- [39] Bjerklin K, Guitirokh CH. Maxillary incisor root resorption induced by ectopic canines. *Angle Orthod*. 2011;81(5):800–806. doi: [10.2319/011311-23.1](https://doi.org/10.2319/011311-23.1).
- [40] Koivisto J, Kiljunen T, Tapiovaara M, et al. Assessment of radiation exposure in dental cone-beam computerized tomography with the use of metal-oxide semiconductor field-effect transistor (MOSFET) dosimeters and Monte Carlo simulations. *Oral Surg Oral Med Oral Pathol Oral Radiol*. 2012;114(3):393–400. doi: [10.1016/j.oooo.2012.06.003](https://doi.org/10.1016/j.oooo.2012.06.003).
- [41] ICRP. Diagnostic reference levels in medical imaging. *Ann. ICRP*. 2017;46(1) ICRP Publication 135